Temperature-Memory Effect of Copolyesterurethanes and their Application Potential in Minimally Invasive Medical Technologies

*Karl Kratz, Ulrike Voigt, and Andreas Lendlein**

Minimally invasive surgery often requires devices that can change their geometry or shape when placed inside the body. Here, the potential of thermoplastic temperature-memory polymers (TMP) for the design of intelligent devices, which can be programmed by the clinician to individually adapt their shifting geometry and their response temperature T_{sw} to the patient´s needs, is explored. Poly(ω-pentadecalactone) as hard segments and poly(ε-caprolactone) segments acting as crystallizable controlling units for the temperature-memory effect (TME) are chosen to form multiblock copolymers PDLCL. These components are selected according to their thermal properties and their good biocompatibility. Response temperatures obtained under stress-free and constant strain recovery can be systematically adjusted by variation of the deformation temperature in a temperature range from 32 °C to 65 °C, which is the relevant temperature range for medical applications. The working principle of TMP based instruments for minimally invasive surgical procedures is successfully demonstrated using three temperature-memory catheter concepts: individually programmable TM-catheter, an in-situ programmable TM-catheter, and an intelligent drainage catheter for gastroenterology.

1. Introduction

Biocompatible, stimuli-sensitive materials, have attracted tremendous interest for biomedical applications such as intelligent medical devices or controlled drug delivery systems.[1–4] In this context shape-materials such as shape-memory alloys (SMA)[5,6] or shape-memory polymers (SMP)[7–11] and their composites are an especially promising class of candidate materials, as they have the capability to perform self-sufficient, pre-defined shape shifts. SMP-based implants can be inserted in a compact shape via a minimally invasive surgery and unfold to their application relevant shape in the body. So far, various thermo-sensitve SMP-based medical devices are being explored for applications such as aneurysm treatment,[12] cloth removal,[13] stents,[14,15] archwires in orthodontics[16] or dialysis needles.[17] A major breakthrough was achieved by the introduction of multifunctional SMP, which combine shape-memory capability with degradability, as a second surgery for explantation of the device can be avoided in this way. Self-tightening intelligent sutures[18] or multifunctional controlled drug delivery systems[19] are examples for biomedical applications, which are explored on the basis of these multifunctional materials.

Thermosensitive SMPs are polymers, which can be deformed and fixed in a second temporary shape, which remains unchanged until heat is applied resulting in the recovery of the original shape. For creation of the temporary shape, typically a heating-deformation-cooling process called programming is utilized, where the deformation is performed at temperatures above the thermal transition (T_{trans}) of the SMP's switching segment and the fixation of the temporary shape is achieved by cooling to temperatures below T_{trans}, while keeping the deformation stress. Finally, heating of the programmed SMP to temperatures above the response temperature results in the activation of the shape-memory effect.[20,21]

Although substantial progress was achieved in the development of SMP systems for medical applications with response temperatures between room temperature or temperatures slightly above body temperature, the currently reported materials do not allow adaptation of the switching temperature (T_{sw}), the characteristic temperature related to shape change during programming. Therefore, a biocompatible polymer material will be required, which allow an accurate and easily adjustment of the shifting geometry as well as T_{sw} according to the individual requirements by the surgeons directly in the operating theatre.

The recently introduced temperature-memory technology might be a promising approach to reach the above mentioned goal. A temperature-memory effect (TME) is the capability of a polymer to remember the temperature, where it was deformed before, by reversing this deformation when this temperature is exceeded again.[22–25] And in this way the class of temperature-memory polymers (TMP) enables the realization of various response temperatures with the same polymer material, without requiring synthesis of a new material.[9]

In contrast to SMPs, temperature-memory polymers exhibit a broad thermal transition ΔT_{trans} (either a glass transition T_g or a melting transition T_m)[22,23,25] and are able to memorize a

Dr. K. Kratz, Dr. U. Voigt, Prof. A. Lendlein
Center for Biomaterial Development
and Berlin-Brandenburg Center for Regenerative Therapies
Institute of Polymer Research
Helmholtz-Zentrum Geesthacht
Kantstr. 55, 14513 Teltow, Germany
E-mail: andreas.lendlein@hzg.de

DOI: 10.1002/adfm.201200211

deformation temperature (T_{deform}) within ΔT_{trans} applied during a specific thermomechanical treatment called temperature-memory creation procedure (TMCP). The temperature-memory capability of such polymers is a result of the fact that the temporary shape is solely fixed by the polymer chains, which are in the rubbery state at T_{deform}. The so established temporary shape remains stable until the fixing domains start to get flexible, when the material is heated again to T_{deform} and in this way allowing the recovery of the original shape.[22,25,26] The high accuracy of the TME reported for recently introduced TMPs with crystallisable controlling units in combination with a small recovery temperature interval (ΔT_{rec}) for completion of the shape change makes TMPs with crystallisable controlling units very attractive for biomedical applications as minimally invasive surgical devices.

Here, we report on a thermoplastic elastomer based on biocompatible polymer segments and a set of temperature-memory (TM) demonstrator devices. Our structural concept for the thermoplastic TMP is a multiblock copolymer consisting of two different crystallizable segments. The hard segments associated to the highest melting temperature determine the permanent shape of the material. The second type of crystallizable segment acts as TME controlling segments. The related melting temperature range should be lower than for the hard segment T_m-range, but at the same time both temperature ranges should partly overlap.

In this way the hard segments can support the TME by formation of crystallites in the upper temperature range of the deformation temperature T_{deform}. Another essential selection criterion of the melting temperature ranges is that the resulting response temperatures, which should be adjustable, are in the desired clinically relevant temperature range.

The multiblock copolymers (named PDLCL) were synthesized by co-condensation of two segment forming macrodiols and an aliphatic diisocyanate according to the method described in.[27] A biocompatible poly(ε-caprolactone)diol (PCL)[28] macromer with a melting temperature (T_m) slightly above body temperature was selected as crystallizable switching segment and biocompatible poly(ω-pentadecalactone) (PPDL)[29] was selected as hard segment forming component.

The temperature-memory properties of the prepared copolyesterurethanes were explored using cyclic, thermomechanical tests consisting of a TMCP where the TME is created by variation of T_{deform}, followed by a recovery module either under stress-free conditions or constant strain conditions for determination of the response temperatures.

Finally, the applicability of such biocompatible temperature-memory thermoplastics was investigated using three temperature-memory catheter concepts.

2. Results and Discussion

2.1. Thermoplastic Temperature-Memory Polymers

A series of biocompatible copolyesterurethanes containing crystallizable switching and hard segments was synthesized by co-condensation of two macrodiols with an aliphatic diisocyanate.[27] In this study PPDL-diol with an apparent average molecular weight of M_n (*app*) = 5600 g mol^{-1} and a T_m = 91 °C, which was prepared by ring-opening polymerization of ω-pentadecalactone with ethylene glycol as initiator was utilized. A crystallizable switching segment was realized by incorporation of poly(ε-caprolactone) segments (PCL, M_n = 3000 g mol^{-1}, T_m = 43 °C). The resulting copolyesterurethanes were named PDLCL. This chemical structure is displayed in Supporting Information Figure S1. In this study the impact of the hard segment content on the temperature-memory capability of the thermoplastics was investigated by variation of the PPDL hard segment contents in the range from 30 wt% to 60 wt%.

The composition (PPDL content) of the copolyesterurethanes was confirmed by ^{1}H-NMR from the signals at δ = 1.25 ppm (PPDL) and δ = 1.39 ppm (PCL) as described in Supporting Information Method 1. The characteristic thermal and mechanical properties of the different PDLCL materials were reported in[27] and are summarized in Supporting Information Table S1. For all multiblock copolymers, two melting transitions (T_m) as well as two crystallization transitions (T_c) are observed in the DSC thermograms, which demonstrate the occurrence of crystalline PCL and PPDL domains. The melting transition related to the PCL controlling units covered a temperature range of $\Delta T_m \approx 35$ °C starting from 20 °C with a broad peak having a maximum around $T_{m,PCL}$ = 44 °C, while the peak maximum of the melting transition attributed to the PPDL was observed at $T_{m,PPDL}$ = 81 °C to 86 °C with a $\Delta T_m \approx 35$ °C. From the DSC an overlap of both melting transitions was apparent in the temperature regime from 50 °C to 70 °C. The obtained T_ms were almost independent from the composition of the PDLCL material. Furthermore, in dynamic mechanical analysis at varied temperature (DMTA) measurements, a glass transition was observed as maximum of the tanδ-temperature-curve. $T_{max,\delta}$ was in the range from −33 °C to −22 °C, whereby $T_{max,\delta}$ was found to increase with increasing PPDL hard segment content. Therefore, the glass transition might be attributed to a mixed amorphous phase. The evaluation of the temperature-memory capability of PDLCL was performed in the melting temperature range of the PCL segments from 25 °C to 55 °C.

The influence of variations of the hard segment contents on structural changes was examined by determining the overall degree of crystallinity (DOC) via wide angle X-ray scattering (WAXS). Here, the isomorphous crystal structure of poly(ε-caprolactone) and poly(ω-pentadecalactone)[30–34] caused an overlapping of appropriate diffraction peaks from PCL and PPDL and the DOC could not be separated into fractions assigned to these components. The obtained DOC values for the prepared copolyesterurethanes varied from 33 ± 1% to 39 ± 1%, whereby the lowest DOC was observed for PDLCL050 containing similar weight contents of PPDL and PCL macrodiols in the starting material mixture (see Supporting Information Table S1).

2.2. Temperature-Memory Creation Procedure

The concept for creating a temperature-memory capability of the prepared copolyesterurethanes with crystallizable switching and hard segments was applying a temperature-memory creation procedure (TMCP), where the deformation at different T_{deform} should determine the memorized response temperatures T_{sw}

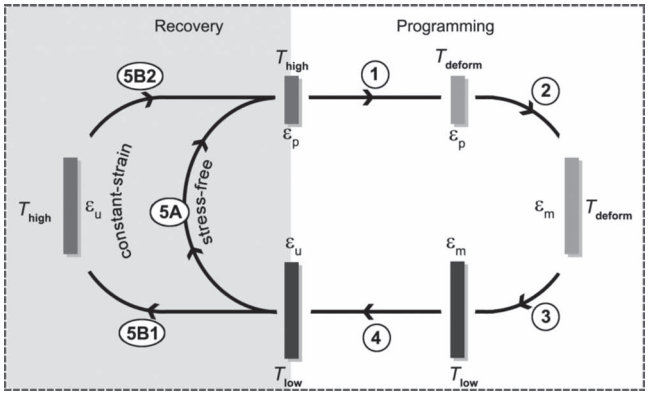

Figure 1. Schematic representation of a cyclic, temperature-memory test consisting of a temperature-memory creation procedure (TMCP) and recovery modules under stress-free and constant strain conditions. The different gray shades of the sample illustrates the applied temperatures: T_{high} (gray), T_{deform} (light gray) and T_{low} (dark gray). Steps 1–4 represent TMCP: cooling from T_{high} to T_{deform} (step 1), elongation from ε_p to ε_m at T_{deform} (step 2) and cooling from T_{deform} to T_{low} under constant stress σ_m (step 3) followed by removing the stress at T_{low} (step 4). Step 5 represents the recovery modules achieved by heating from T_{low} to T_{high}: under stress-free conditions (step 5A) and under constant strain conditions (step 5B1), while the stress is removed to allow recovery at T_{high} (step 5B2).

and $T_{\sigma,max}$. The TMCP should be designed in such a way that the mechanical deformation is predominantly fixed by that fraction of switching segment crystallites or even low melting hard segment fraction having a melting temperature close to T_{deform}.

A schematic representation of a cyclic, temperature-memory test consisting of a multi-step temperature-memory creation procedure (TMCP) and recovery modules under stress-free and constant strain conditions is illustrated in **Figure 1**. In step (1) the test specimen is cooled from T_{high} = 70 °C or 65 °C, which was above $T_{m,PCL}$ and below $T_{m,PPDL}$ to the applied T_{deform}. Step 2 represents the key process of the TMCP, where the deformation to ε_m at T_{deform} is performed. Cooling from T_{deform} to T_{low} under constant stress σ_m (step 3) followed by removing the stress at T_{low} (step 4), whereby T_{low} was chosen below the onset of T_m(PCL), completed the TMCP resulting in the fixed temporary shape ε_u. Recovery under stress-free conditions is achieved via heating from T_{low} to T_{high}, whereby the original shape ε_p is recovered and the switching temperature T_{sw} can be determined as inflection point of the strain-temperature curve.[35] In contrast, during recovery under constant strain conditions (step 5B1), heating from T_{low} to T_{high} is performed at fixed strain, while the recovery stress is monitored, whereby the response temperature $T_{\sigma,max}$ is related to the maximum recovery stress σ_{max}.[35] Finally, removing the stress allows recovering ε_p at T_{high} (step 5B2).

The following demonstration experiment was designed to demonstrate the temperature-memory capability of PDLCL. A pre-elongated (programmed) polymer ribbon serves as thermosensitive switch that activates a LED lamp at predetermined temperatures, while the change in voltage is recorded (**Figure 2** and Supporting Information Video S1). In this experiment a PDLCL040 ribbon was deformed to ε_m = 150% at T_{deform} = 35 °C or 55 °C, while fixation of the temporary shape was achieved by cooling to T_{low} = −10 °C. The shape recovery of the PDLCL040 ribbon programmed at T_{deform} = 35 °C activates the switch at 39 °C, while for the PDLCL040 ribbon programmed at T_{deform} = 55 °C, the switch is not activated until a temperature of 54 °C is reached. This experiment impressively demonstrated the temperature-memory capability of PDLCL materials after application of TMCP.

To survey our assumption that step 2 during TMCP is the key process, which is responsible for creation of TME, wide angle X-ray scattering (WAXS) experiments were performed to explore the influence of the different TMCP steps on the crystallinity of the material. All investigated samples (PDLCL040) exhibit similar DOC values of about 55% after finishing TMCP independent from the applied T_{deform}. DOC increased during each subsequent step of TMCP. A major increase in DOC from values of 21%-28% to values of 37%–50% was obtained after step 2 (deformation at

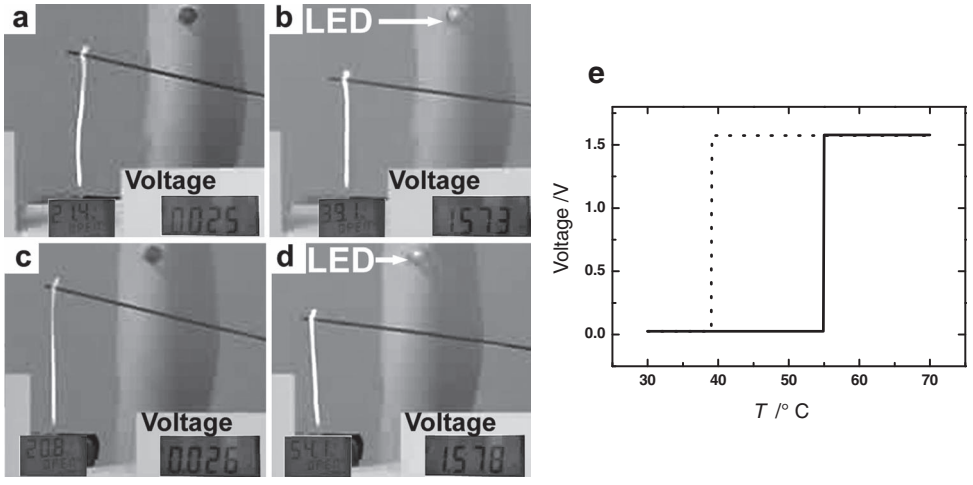

Figure 2. Photograph series of temperature-memory demonstration experiment, where a polymer ribbon fabricated from PDLCL040 programmed at T_{deform} = 35 °C (a,b) or 55 °C (c,d) serves as thermosensitive switch that activates a LED lamp at predetermined temperatures, while the change in voltage is recorded (e); T_{deform} = 35 °C (dotted line) and T_{deform} = 55 °C (solid line).

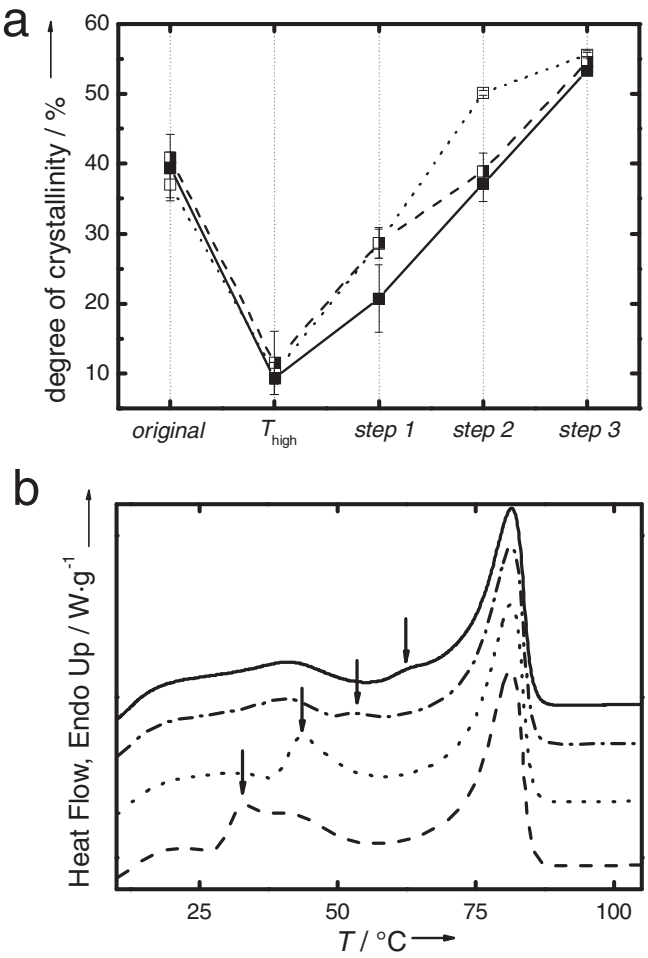

Figure 3. a) Change in overall degree of crystallinity (DOC) determined via wide angle X-ray scattering (WAXS) for PDLCL040 programmed at different T_{deform} at different steps during TMCP. The WAXS experiments were performed at room temperature (original) before starting TMCP, at T_{high} = 70 °C, after cooling from T_{high} to T_{deform} (step 1), after elongation to ε_m at T_{deform} (step 2) and after cooling to T_{low} under constant stress (step 3). Dotted line with open squares: T_{deform} = 35 °C; dashed-dotted line with half-filled squares, T_{deform} = 45 °C; solid line with filled squares, T_{deform} = 55 °C. b) DSC thermograms obtained for PDLCL050. Heating curves from T_{low} to T_{high} (corresponding to step 5A, stress free recovery) after thermal treatment in analogy to temperature-memory programming, but without application of external stress. First cooling from T_{high} to T_{deform} with a cooling rate of 10 K min^{-1} and afterwards keeping the samples at T_{deform} for 10 min. The included arrows indicate the shift of the melting temperature related to the temperature-memory switching segment. Solid line: T_{deform} = 55 °C; dashed-dotted line: T_{deform} = 45 °C; dotted line: T_{deform} = 35 °C; dashed line: T_{deform} = 25 °C.

T_{deform}) (**Figure 3**a), whereby strain-induced crystallization was found most pronounced for T_{deform} = 35 °C.

In addition, DSC experiments were carried out, where the samples were exposed solely to the thermal treatment applied during TMCP, meaning without mechanical deformation (see Experimental section). The thermograms obtained in the following reheating step from T_{low} to T_{high} are displayed in Figure 3b for different T_{deform}. While $T_{m,PPDL}$ is independent from the applied T_{deform}, $T_{m,PCL}$ increased with increasing T_{deform} up to T_{deform} = 45 °C, whereby for T_{deform} > 25 °C two peaks could be observed for the PCL related melting transition. This effect might be attributed to isothermal crystallization,[36] at T_{deform} occurring during step 1. For T_{deform} = 55 °C the formation of a shoulder of the PPDL melting peak in the range of 60 °C to 70 °C was observed, which might be caused by annealing of PPDL crystallites. Subsequent cooling from T_{deform} to T_{low} leads to a second melting peak attributed to the crystallization of PCL segments, which are amorphous at T_{deform}. Therefore, we can conclude that besides the prominent strain-induced crystallization also thermally-induced crystallization processes could contribute to the formation of crystallites acting as reversible crosslinks, and fixing the temporary shape during TMCP.

An alternative thermomechanical experiment was carried out to demonstrate that the deformation at T_{deform} within the ΔT_m of the PCL switching segment is necessary for creation of TME. In this experiment a PDLCL040 sample was first deformed at T_{high} = 65 °C or 70 °C and then cooled to T_{deform} and subsequently to T_{low} allowing isothermal crystallization at both temperatures. Three subsequent cycles under stress-free recovery conditions were performed, in which T_{deform} was varied from 55 °C to 25 °C (2nd cycle) and again to 55 °C (3rd cycle). T_{sw}, which was determined in each cycle, remained constant at 56 °C and was not influenced by variation of T_{deform} (Supporting Information Figure S2). This experiment demonstrates impressively that a solely thermal treatment at T_{deform} is not sufficient to influence T_{sw}. A specific thermomechanical conditioning is required to realize a TME, which allows memorizing T_{deform}.

2.3. Quantification of Temperature-Memory Properties

Temperature-memory properties of PDLCL were investigated by cyclic, thermomechanical tensile tests carried out on a tensile tester equipped with a thermo chamber, a detailed description is given in the Experimental section. Each cycle consists of TMCP where the temperature-memory is programmed and a recovering module where the response temperature is determined.

Two different recovery modules were applied: stress-free and constant strain conditions. Under stress-free conditions (σ = 0 MPa) TME is quantified by determination of T_{sw}. Under constant strain conditions, where the recovery stress is monitored, the response temperature $T_{\sigma,max}$ can be obtained at the maximum recovery stress σ_{max} generated during the TME (for details see Experimental section). Typical results obtained for PDLCL040 under constant strain or stress-free conditions are displayed in **Figure 4** for T_{deform} = 25 °C (black line) and 55 °C (gray line). The corresponding response temperatures were found to be in the range of the applied deformation temperatures (T_{deform} = 25 °C, T_{sw} = 34 °C, $T_{\sigma,max}$ = 47 °C; T_{deform} = 55 °C, T_{sw} = 53 °C, $T_{\sigma,max}$ = 65 °C), which demonstrates the successful temperature-memory functionalization of the copolyesterurethanes by application of TMCP.

A key characteristic for the TME is the influence of T_{deform} on $T_{\sigma,max}$ and T_{sw}, which is shown in **Figure 5** for PDLCL050. In a series of experiments (each three cycles) with PDLCL050 T_{deform} was varied, while all other parameters were kept constant

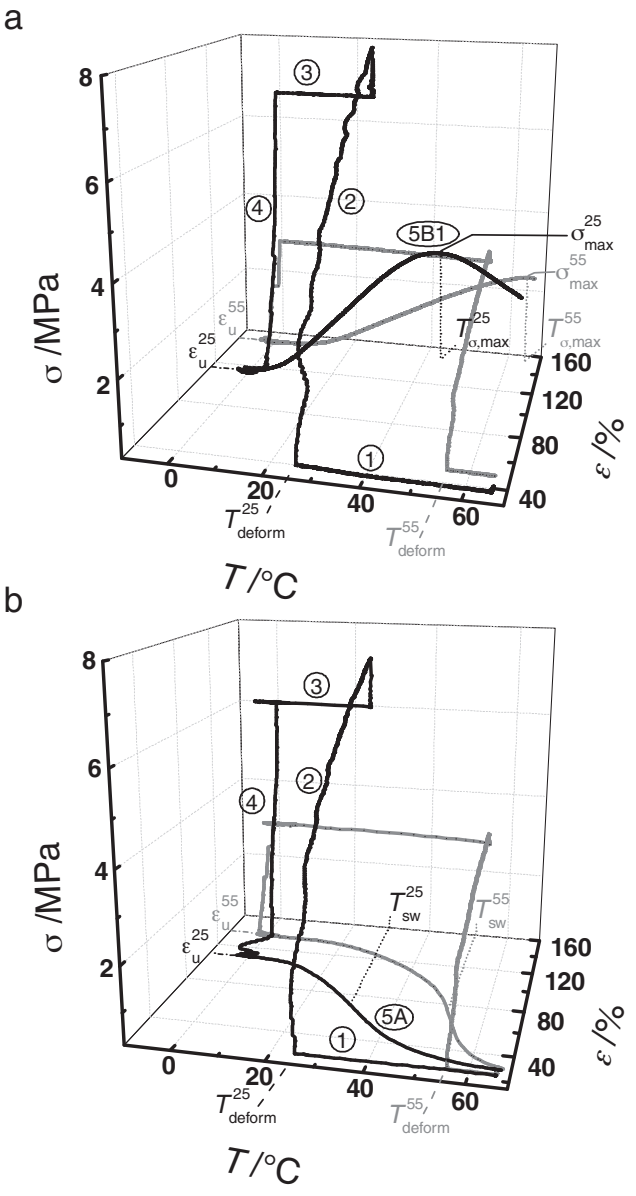

Figure 4. Quantification of TME by cyclic, thermomechanical tests. The graphs show the second test cycle including *TMCP* (step 1–4), and recovery under stress-free conditions (step 5A) [a] as well as under constant strain control (step 5B1) [b] with ε_m = 150%, T_{low} = 0 °C and T_{high} = 65 °C for PDLCL040. Black line: T_{deform} = 25 °C and gray line: T_{deform} = 55 °C.

(ε_m = 150%, T_{low} = 0 °C). T_{sw} as well as $T_{\sigma,max}$ are almost linearly increasing with rising T_{deform}. The corresponding recovery curves obtained under stress-free and constant strain conditions are displayed in Supporting Information Figure S3. In how far a thermomechanical treatment previous to the current TMCP can influence the temperature-memory behavior, especially the observed $T_{\sigma,max}$ was investigated in the following for PDLCL050. A first experiment consists of four cycles where T_{deform} was increased by 10 K with each cycle starting from 25 °C. In a second experiment also consisting of four cycles, T_{deform} was decreased by 10 K with each cycle starting from 55 °C. In both

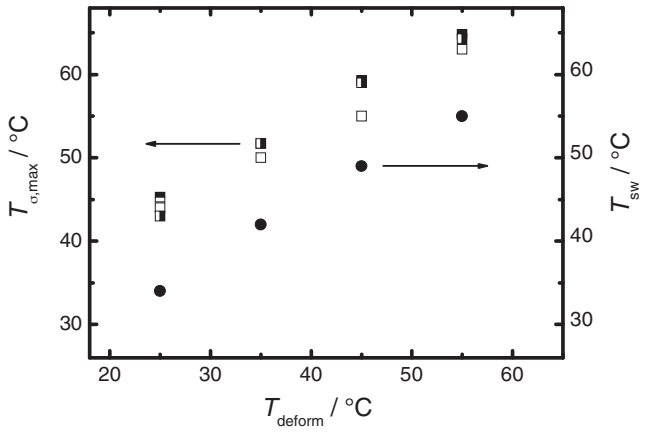

Figure 5. $T_{\sigma,max}$ and T_{sw} as a function of T_{deform} determined in cyclic thermomechnical tests for PDLCL050 with: ε_m = 150%, T_{low} = 0 °C and T_{high} = 70 °C, horizontal, half-filled squares: $T_{\sigma,max}$, four subsequent cycles: T_{deform} = 55 °C - 45 °C - 35 °C - 25 °C, open squares: $T_{\sigma,max}$ each three cycles at T_{deform} = 25 °C or 35 °C or 45 °C or 55 °C, vertical half-filled squares: $T_{\sigma,max}$, four subsequent cycles: T_{deform} = 25 °C - 35 °C - 45 °C - 55 °C, filled circles: T_{sw} each three cycles at T_{deform} = 25 °C or 35 °C or 45 °C or 55 °C. The errors for the applied T_{deform} and the determined response temperatures T_{sw} and $T_{\sigma,max}$ were estimated according the accuracy of the thermal chamber to ±1 °C and are represented by the size of the symbols.

experiments, $T_{\sigma,max}$ is only influenced by the current T_{deform} and is highly reproducible for each specific T_{deform}. This independence from the thermal history is a great advantage towards the applicability of this technology.

Further characteristics for the quantification of the temperature-memory effect besides the response temperatures are the shape fixity rate R_f, the shape recovery rate R_r and the recovery stress σ_{max}.[35] Here R_f represents the accuracy of fixing the applied deformation after finishing TMCP, which is defined as the ratio of the tensile total strain after unloading, $\varepsilon_u(N)$ and ε_m according to Equation (1).

$$R_f(N) = \frac{\varepsilon_u(N)}{\varepsilon_m} \quad (1)$$

The shape recovery ratio R_r quantifies how well the original shape has been recovered and is a measure of how far a strain that was applied in the course of the programming is recovered as a result of the TME. The shape recovery ratio R_r is defined as the ratio of the strain in the present (Nth) cycle ε_m–$\varepsilon_p(N)$ and the strain in previous cycle ε_m–$\varepsilon_p(N\text{-}1)$ according to Equation (2).

$$R_r(N) = \frac{\varepsilon_m - \varepsilon_p(N)}{\varepsilon_m - \varepsilon_p(N-1)} \quad (2)$$

The temperature-memory properties achieved for PDLCL materials with different hard segment contents, when deformed at T_{deform} = 55 °C and T_{deform} = 25 °C are summarized in **Table 1**. In all experiments the observed response temperatures were in the range of the applied deformation temperature (T_{deform} = 25 °C: T_{sw} = 32 °C – 34 °C, $T_{\sigma,max}$ = 45 °C–47 °C and at T_{deform} = 55 °C: T_{sw} = 53 ± 1 °C, $T_{\sigma,max}$ = 62 °C–65 °C), demonstrating that the temperature-memory capability is independent from the chemical composition of the copolymers. All copolyesterurethanes exhibited excellent shape fixity rates in the range of R_f = 89%-99%, when deformed at 55 °C, whereby R_f was

Table 1. Temperature-memory properties of copolyesterurethanes PDLCL.

Sample ID[a)]	$R_f(2)$[d)] [%]	$R_f(3)$[d)] [%]	$R_r(2)$[d)] [%]	$R_r(3)$[d)] [%]	$T_{sw}(2)$[e)] [°C]	$T_{\sigma,max}(2)$[e)] [°C]	σ_{max} (2)[e)] [MPa]
PDLCL060[b)]	89 ± 2	89 ± 2	94 ± 2	98 ± 2	53 ± 1	65 ± 1[#]	3.2 ± 0.2
PDLCL050[b)]	93 ± 2	92 ± 2	96 ± 2	98 ± 2	53 ± 1	65 ± 1[#]	2.5± 0.2
PDLCL040[b)]	93 ± 2	93 ± 2	97 ± 2	99 ± 2	53 ± 1	65 ± 1[#]	2.6± 0.2
PDLCL030[b)]	99 ± 2	99 ± 2	97 ± 2	98 ± 2	53 ± 1	62 ± 1[#]	1.9± 0.2
PDLCL060[c)]	70 ± 2	69 ± 2	96 ± 2	96 ± 2	32 ± 1	46 ± 1*	2.8± 0.2
PDLCL050[c)]	70 ± 2	69 ± 2	95 ± 2	96 ± 2	32 ± 1	45 ± 1	3.2± 0.2
PDLCL040[c)]	71 ± 2	71 ± 2	91 ± 2	94 ± 2	34 ± 1	47 ± 1	3.5± 0.2
PDLCL030[c)]	71 ± 2	71 ± 2	98 ± 2	98 ± 2	33 ± 1	45 ± 1	3.2± 0.2

[a)]The three-digit number gives the weight content of PPDL in wt% related to the starting material composition of PPDL and PCL diols; [b)]Programming at T_{deform} = 55 °C, recovery at T_{high} = 65 °C ($^{\#}T_{high}$ = 70 °C); [c)]Programming at T_{deform} = 25 °C, recovery at T_{high} = 65 °C ($^{*}T_{high}$ = 55 °C); [d)]R_r (shape recovery rate), R_f (shape fixity rate) and T_{sw} determined by cyclic, thermomechanical experiments for cycle N = 2 and N = 3 applying the recovery module under stress-free conditions; [e)]$T_{\sigma,max}$ and σ_{max} resulting from recovery experiments under constant strain control for cycle N = 2. In all experiments ε_m = 150%, T_{low} = 0 °C are fixed. The denoted errors for the single experiments are estimated to ± 2% for R_r and R_f, and ± 1 °C for T_{sw} and $T_{\sigma,max}$.

found to increase systematically with increasing PCL switching segment content. In contrast significant lower R_f values around 70%–77% were obtained for samples functionalized at T_{deform} = 25 °C, which were independent from the materials composition. The difference in the observed R_f at different T_{deform} can be explained by a higher rubber elastic relaxation in the cold drawing process at 25 °C compared to the situation at T_{deform} = 55 °C.

Excellent shape recovery rates R_r in the range of R_r = 91%-98% were achieved for all samples independent from the applied deformation temperature. Recovery experiments under constant strain conditions showed a moderate decrease of σ_{max} generated during TME with increasing T_{deform} from 25 °C to 55 °C for all copolyesterurethanes (see Table 1). While σ_{max} at T_{deform} = 25 °C was almost independent from the copolymer composition at T_{deform} = 55 °C an increase in σ_{max} with rising PPDL content was observed, which can be attributed to an increasing contribution of PPDL domains to the TME.

To prove our concept that the realization of TME in thermoplastic polymers with crystallizable switching segments requires a crystallizable hard segment, which has a similar crystal structure, whereby the melting transitions of both segments should partly overlap, and in this way should support the TME by formation of crystallites in the upper temperature range of the response temperature in combination with a specific TMCP, we investigated the temperature-memory capability of established degradable and biocompatible thermoplastic copolyesterurethanes, which show no overlap of the melting transitions related to the switching and hard segments. Here, we chose a multiblock copolymer containing poly(*p*-dioxanone) (PPDO) hard segments and poly(ε-caprolactone) switching segments with a PCL content of 48 wt-% named PDC048, which was prepared according to the method described by Lendlein et al.[18] (Supporting Information Method S2). The DSC heating curve obtained in the 2nd heating run is displayed in Supporting Information Figure S4 in comparison to the DSC thermogram of PDLCL050. Here no overlap of the PCL and PPDO melting transitions could be observed, although crystallization of PPDO occurred when the temperature reaches the onset of the PCL melting transition. In contrast, the PDLCL050 exhibited an overlap of the PCL and PPDL melting transitions in the temperature range from 50 °C to 70 °C. The temperature-memory experiments for PDC048 (Supporting Information Method S3) did not show a pronounced TME. Only a slight shift in T_{sw} from 27 °C to 36 °C could be achieved, when T_{deform} was varied from 15 °C to 55 °C (see Supporting Information Figure S5). We assume that the absence of TME capability for PDC048 can be attributed to the missing overlap of the melting transitions of PCL and PPDO, which might be a result of a better phase separated morphology of PDC048 in comparison to PDLCL050. Further indications for a difference in the phase morphology of PDC and PDLCL copolyesterurethanes are the observation of two separated glass transitions in case of PDC,[18] while for PDLCL a mixed glass transition is obtained[27] or the fact that the WAXS diffraction peaks from PCL and PPDL could not be separated, whereas for PDC a separation of the PPDO and PCL signals was reported.[37] Therefore, we conclude that the crystalline PPDO segments could not contribute to the temperature-memory capability of PDC048 and a TME could only be achieved within the melting temperature range of the crystalline PCL.

The feasibility of the TMP technology for intelligent medical devices, such as instruments for minimally invasive surgical procedures, was explored. For this purpose three temperature-memory catheter (TM-catheter) concepts (1st: individually programmable TM-catheter, 2nd: in-situ programmable TM-catheter and 3rd: intelligent drainage catheter) fabricated from PDLCL050 were investigated as demonstration devices.

The individually programmable TM-catheter will enable the surgeon to adapt the catheters geometry and response temperature according to the individual needs of the patient in situ in the surgical procedure. With such a TM-catheter the operator can predetermine the response temperature T_{sw} of the catheter by the choice of T_{deform} applied during TMCP. In the demonstration experiment an originally 90° bent TM-catheter was temporary straightened at T_{deform} = 37 °C or 49 °C. The working principle of the individually programmable TM-catheter is

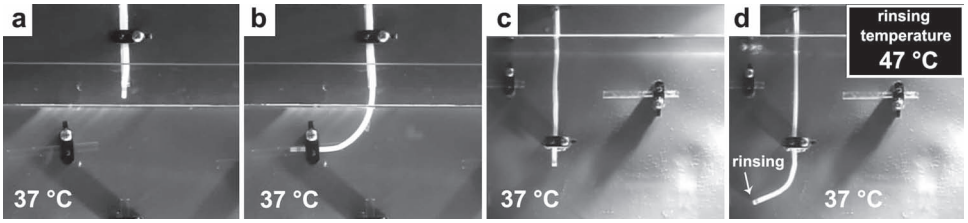

Figure 6. Photograph series of an individually programmable TM-catheter fabricated from PDLCL050. The programmed catheter is introduced in a water bath at 37 °C. In addition, the catheter can be rinsed with warmed water (here 47 °C). The images (a,b) show that the TM-catheter, which was programmed at 37 °C, bends when introduced in the 37 °C warm water bath. The photographs (c,d) illustrate that the TM-catheter, which was programmed at 49 °C, remains form stable at body temperature. On demand movement (bending) was initiated by rinsing with 47 °C warm water.

visualized in Supporting Information Video S2 and the photo series displayed in **Figure 6**a–d. While the catheter, which was functionalized at 37 °C bent when introduced into the 37 °C warm water bath, the same catheter was form stable at body temperature when TMCP was performed at T_{deform} = 49 °C before and could only be activated by rinsing with warm water of the same temperature (47 °C) through the catheter. Here, a response temperature <50 °C was selected as suitable temperature, which could be applied for a short time period inside the body according to work about a laser-activated intravascular thrombectomy device reported by Maitland et al.[38]

As a second TM-catheter concept, we explored an in-situ programmable TM-catheter (Supporting Information Video S3 and **Figure 7**a–d) to demonstrate the capability of programming a TME inside the human body, which might be applied for temporary fixation of an implant, and can be removed afterwards on demand by activation of the TME. Here, the originally 90° bent TM-catheter was temporary straightened at T_{deform} = 37 °C. Bending was induced by heating to 37 °C in a water bath. In the next step a further temperature-memory functionalization of the catheter, which was kept at body temperature, was performed by rinsing the catheter with 49 °C warmed water, expanding the catheter tail at T_{deform} = 49 °C and subsequent cooling by rinsing with water of 10 °C while keeping the deformation. After removal of the expansion device the temporary expanded catheter tail is achieved and in this way the TM-catheter was fixed and could not be pulled out. Reheating the catheter to 49 °C via rinsing again with warmed water caused the shrinkage of the catheter tail and therefore the in-situ programmed device could be removed easily.

Finally, the applicability of the TMP technology was explored as an intelligent drainage catheter system for gastroenterological applications. The intelligent drainage catheter was designed in such a way that both a TME controlled pigtail formation as well as on demand opening of drainage pores can be realized. The system consisted of a TM-catheter, which was originally shaped as catheter with a pigtail winded in two turns and three opened drainage pores, and a conventional PTFE-tube inserted into the TM-catheter. The intelligent drainage catheter was programmed by application of a two step TMCP, where the pores were closed and a single winded pigtail was created at T_{deform} = 60 °C in step one, while the whole catheter was straightened at T_{deform} = 37 °C in the final programming step. When heated to body temperature in a water bath a pigtail with a single turn was formed. A further pigtail winding was achieved as well as a first pore was opened by rinsing the TM-catheter via an inserted PTFE- tube, which was placed above the first pore, with 60 °C warm water. Pulling back the PTFE-tube, while continuously rinsing with 60 °C warm water, resulted in opening of the two other pores. The working principle of the intelligent drainage catheter system is visualized in Supporting Information Video S4 and the photo series displayed in **Figure 8**a–d.

3. Conclusion

A family of thermoplastic copolyesterurethanes PDLCL consisting of biocompatible crystallizable PCL switching and PPDL hard segments was introduced exhibiting a pronounced temperature-memory effect. In this way T_{sw} as well as $T_{\sigma,max}$

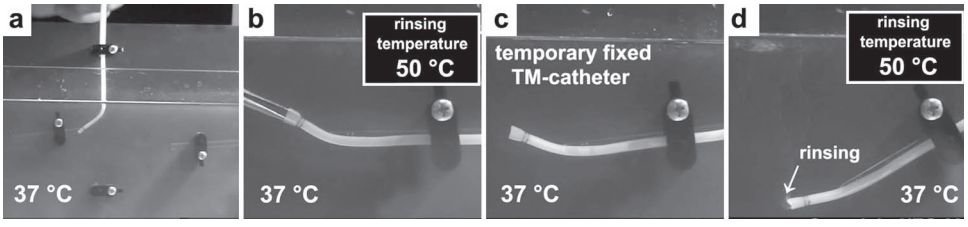

Figure 7. Photograph series of an in-situ programmable TM-catheter prepared from PDLCL050. A TM-catheter programmed at 37 °C before, bent first when heated to body temperature (a). Afterwards the catheter tail is programmed in-situ by expanding the tail at T_{deform} = 49 °C, which was reached by rinsing the catheter with warmed water (b) and subsequent cooling by rinsing the catheter with cold water (10 °C), while keeping the strain. After removal of the expansion device a TM-catheter with a temporary expanded tail is achieved, which could not be pulled out (c). Reheating the catheter to 50 °C via rinsing with warmed water caused a shrinkage of the temporary expanded catheter tail and the device could be removed easily (d).

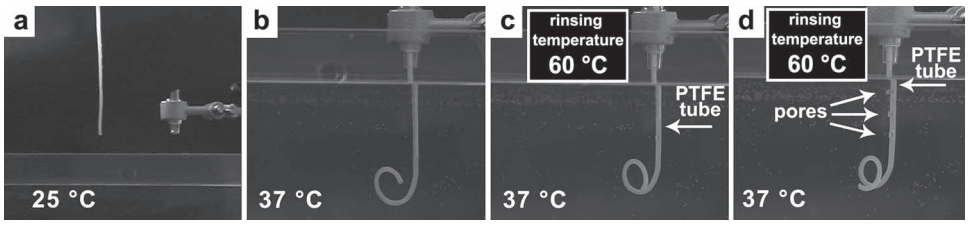

Figure 8. Photograph series of a pigtail TM-catheter containing three pores for application as intelligent drainage catheter fabricated from PDLCL050. The TM-catheter was initially straightened up to one pigtail at T_{deform} = 60 °C, while a complete straightening was performed at T_{deform} = 37 °C. The programming (closing) of the pores was conducted at T_{deform} = 60 °C. (a). When heated to body temperature the catheter tip turned into a single coil (b). A further pigtail winding was achieved and the first pore was opened by rinsing the TM-catheter with 60 °C warm water via an inserted PTFE-tube, whereby the tube opening was located in between the first and the second pore of the catheter. (c). Finally, pulling back the PTFE-tube while continuously rinsing with 60 °C warm water resulted in opening of the remaining two pores (d).

could be controlled systematically in the range from 32 °C to 65 °C by variation of T_{deform} during TMCP. The high accuracy of the TME as well as a rather simple programming technology, which could be performed by the surgeons in the operating theatre as well as the opportunity to perform in-situ programming inside the human body makes such biocompatible polymers promising candidate materials for application in minimally invasive medical technologies.

The TME working principle was successfully demonstrated for temperature-memory catheters that could be utilized for custom-fit placement of the device or temporary fixation. Finally, an intelligent drainage pigtail catheter for gastroenterology was explored.

As the presented temperature-memory copolyesterurethanes will allow the realization of different medical devices with the same polymer material, only a single approval process is required, which currently represents a major hurdle for realization of novel medical devices.

In a next step, the outcome of this work needs to be transferred into processes suitable for a small series production, which is required for preclinical and clinical evaluation of such intelligent catheters.

4. Experimental Section

Synthesis: Copolyesterurethanes were prepared as reported previously.[27] In the following, the synthesis is exemplarily described for PDLCL040: 20 g PPDL-diol (M_n = 5600 g mol^{-1} and T_m = 91 °C, which was prepared by ring-opening polymerization of ω-pentadecalactone with ethylene glycol as initiator),[27] 30 g PCL-diol (M_n = 3000 g mol^{-1} and T_m = 43 °C; Solvay, Warringthon, UK) and 4,4 g 2,2,(4),4-trimethylhexanediisocyanat (TMDI, purity >99%, Fluka, Taufkirchen, Germany) were reacted in 1,2-dichlorethane at 80 °C for 10 days. The product was obtained by precipitation in methanol at –10 °C (Yield 91%).

Differential Scanning Calorimetry: DSC experiments were performed on a Netzsch DSC 204 Phoenix (Selb, Germany). Thermal characterization comprised heating from 20 °C to 150 °C, then cooling down to –100 °C and reheating to 150 °C (2nd heating). Thermal transitions were determined from the second heating run. All heating and cooling procedures were performed with a constant heating and cooling rate of 10 K min^{-1}. For TME related DSC experiments the samples were first cooled from room temperature to –100 °C and then heated to 150 °C applying a constant heating and cooling rate of 10 K min^{-1}. After cooling to 70 °C (T_{high}) with 10 K min^{-1} and isothermal storage for 10 min, the samples were rapidly cooled to the desired T_{deform} with 50 K min^{-1}. The isothermal conditioning at T_{deform} is performed for 10 min followed by cooling down to 0 °C (T_{low}) with 50 K min^{-1} and subsequent isothermal treatment for 10 min. Thermal transitions and melting enthalpies were determined while heating to 150 °C with a heating rate of 10 K min^{-1}.

Wide Angle X-ray Scattering: The WAXS measurements were carried out on a X-ray diffraction system Bruker D8 Discover with a two-dimensional detector from Bruker AXS (Karlsruhe, Germany). The X-ray generator, producing copper K-alpha radiation with a wavelength of 0.154 nm, was operated at a voltage of 40 kV and a current of 40 mA. A graphite monochromator and a pinhole collimator with an opening of 0.8 mm defined the optical and geometrical properties of the beam. A custom-built setup with a hot air gun and a stretching device with micrometer screws allowed X-ray diffraction measurements to be performed at different stages during the programming cycle of the samples. While a thermocouple touching the sample enabled taking diffraction images at defined temperatures ranging from 30 to 70 °C (±4 °C), the stretching device enabled the required 150% elongation of the sample. Samples with a thickness of about 0.5 to 1 mm were illuminated for 2 min in transmission geometry and the diffraction images were collected at a sample-to-detector distance of 15 cm. The two-dimensional diffraction images were integrated to obtain plots with intensity versus diffraction angle (2-theta). These profiles were analyzed using the Bruker software TOPAS to determine the degree of crystallinity, which is the ratio between the area of crystalline peaks and the total area below the diffraction curve (area of crystalline peaks plus area of the amorphous halo).

Cyclic Thermomechanical Tests for Determination of Temperature-Memory Properties: Cyclic, thermomechanical tensile tests were performed on the tensile tester Zwick Z1.0 or Z005 (Zwick, Ulm, Germany) equipped with a thermo chamber and a temperature controller (Eurotherm Regler, Limburg, Germany). Test specimens were produced with a polymer press (type 200 E, Dr. Collin, Ebersberg, Germany) at 100 °C under a pressure of 90 bar for 4 min. The film thickness was typically between 0.4 and 0.6 mm. Specimen type 1BB according to European Standard for tensile test (DIN EN ISO1BB) were cut with a punching tool, l_0 = 20 mm, width 2 mm.

Each cycle consisted of a TMCP module for creating the temperature-memory capability and a recovery module where T_{sw} (stress-free conditions) or $T_{\sigma,max}$ (constant strain conditions) was determined. Every recovery module was completed by a waiting period of 10 min. The cycles were repeated three times per test. In all thermomechanical tests the first cycle was applied as pre-conditioning procedure, while the data were determined in the 2nd and 3rd cycle.

TMCP-module: The specimen was cooled form T_{high} (65 °C or 70 °C) to T_{deform}, and deformed at T_{deform} to ε_m = 150%, where the strain was kept constant for 5 min to allow relaxation. In the following the sample was cooled down to T_{low} = 0 °C and equilibrated for 10 min at T_{low}. Finally, the stress was removed and the elongation of the sample in the temporary ε_u was determined.

Recovery Under Stress-Free Conditions-Module: The recovery of the original shape was induced by heating the programmed sample to T_{high} (65 °C or 70 °C) with a heating rate of 2 K min^{-1} under stress-free condition. The tension-free strain value after the completion of the recovery process ε_p was determined as well as T_{sw}, which was obtained as inflection point in the strain-temperature recovery curve.

Recovery Under Constant Strain Conditions-Module: This recovery module under constant strain conditions was carried out after applying the TMCP module for the determination of the maximum stress σ_{max} and the corresponding temperature $T_{\sigma,max}$. The sample was heated up to T_{high} with a heating rate of 2 K min^{-1}, while the strain was kept constant at ε_u. Both σ_{max} and $T_{\sigma,max}$ were determined at the maximum value of σ in the stress-temperature recovery curve. After reaching T_{high}, the strain constraint was removed and switched to $\sigma = 0$ MPa allowing the sample to recover its original shape.

Supporting Information

Supporting Information is available from the Wiley Online Library or from the author.

Acknowledgements

The authors thank Dr. Wolfgang Wagermaier for conducting the WAXS experiments of the copolyesterurethanes. The authors are thankful to the clinical experts Carsten Tschoepe and Dietlind Zohlnhoefer-Momm (Department of Cardiology), as well as Martin Zeitz, Christian Bojarski, and Frank Heller (Department of Gastroenterology, Infectiology and Rheumatology), Charité, University Medicine Berlin for discussion about potential medical applications.

Received: January 23, 2012
Revised: March 9, 2012
Published online: April 16, 2012

[1] C. D. H. Alarcon, S. Pennadam, C. Alexander, *Chem. Soc. Rev.* **2005**, *34*, 276.
[2] M. A. C. Stuart, W. T. S. Huck, J. Genzer, M. Muller, C. Ober, M. Stamm, G. B. Sukhorukov, I. Szleifer, V. V. Tsukruk, M. Urban, F. Winnik, S. Zauscher, I. Luzinov, S. Minko, *Nat. Mater.* **2010**, *9*, 101.
[3] C. Alexander, *Nat. Mater.* **2008**, *7*, 767.
[4] J. Jagur-Grodzinski, *Polym. Adv. Technol.* **2010**, *21*, 27.
[5] F. El Feninat, G. Laroche, M. Fiset, D. Mantovani, *Adv. Eng. Mater.* **2002**, *4*, 91.
[6] D. Mantovani, *JOM-J. Min. Met. Mater. Soc.* **2000**, *52*, 36.
[7] P. R. Buckley, G. H. McKinley, T. S. Wilson, W. Small, W. J. Benett, J. P. Bearinger, M. W. McElfresh, D. J. Maitland, *IEEE Trans. Biomed. Eng.* **2006**, *53*, 2075.
[8] A. Lendlein, M. Behl, B. Hiebl, C. Wischke, *Expert Rev. Med. Dev.* **2010**, *7*, 357.
[9] I. V. W. Small, P. Singhal, T. S. Wilson, D. J. Maitland, *J. Mater. Chem.* **2010**, *20*, 3356.
[10] W. Sokolowski, A. Metcalfe, S. Hayashi, L. Yahia, J. Raymond, *Biomed. Mater.* **2007**, *2*, S23.
[11] C. M. Yakacki, K. Gall, *Adv. Polym. Sci.* **2010**, *226*, 147.
[12] W. Small, P. R. Buckley, T. S. Wilson, W. J. Benett, J. Hartman, D. Saloner, D. J. Maitland, *IEEE Trans. Biomed. Eng.* **2007**, *54*, 1157.
[13] W. Small, M. F. Metzger, T. S. Wilson, D. J. Maitland, *IEEE J. Sel. Top. Quantum Electron.* **2005**, *11*, 892.
[14] G. Baer, T. Wilson, D. Maitland, D. Matthews, *J. Invest. Med.* **2006**, *54*, S162.
[15] C. M. Yakacki, R. Shandas, C. Lanning, B. Rech, A. Eckstein, K. Gall, *Biomaterials* **2007**, *28*, 2255.
[16] Y. C. Jung, J. W. Cho, *J. Mater. Sci. Mater. Med.* **2008**.
[17] J. M. Ortega, W. Small, T. S. Wilson, W. J. Benett, J. M. Loge, D. J. Maitland, *IEEE Trans. Biomed. Eng.* **2007**, *54*, 1722.
[18] A. Lendlein, R. Langer, *Science* **2002**, *296*, 1673.
[19] C. Wischke, A. T. Neffe, S. Steuer, A. Lendlein, *J. Controlled Release* **2009**, *138*, 243.
[20] M. Behl, J. Zotzmann, A. Lendlein, *Adv. Polym. Sci.* **2010**, *226*, 1.
[21] T. Xie, *Polymer* **2011**, *52*, 4985.
[22] K. Kratz, S. A. Madbouly, W. Wagermaier, A. Lendlein, *Adv. Mater.* **2011**, *23*, 4058.
[23] P. Miaudet, A. Derre, M. Maugey, C. Zakri, P. M. Piccione, R. Inoubli, P. Poulin, *Science* **2007**, *318*, 1294.
[24] J. Cui, K. Kratz, M. Heuchel, B. Hiebl, A. Lendlein, *Polym. Adv. Technol.* **2011**, *22*, 180.
[25] T. Xie, *Nature* **2010**, *464*, 267.
[26] L. Sun, W. M. Huang, *Soft Matter* **2010**, *6*, 4403.
[27] K. Kratz, U. Voigt, W. Wagermaier, A. Lendlein, *Mater. Res. Soc. Symp. Proc.* **2009**, *1140*, 17.
[28] M. A. Woodruff, D. W. Hutmacher, *Prog. Polym. sci.* **2010**, *35*, 1217.
[29] J. Liu, Z. Jiang, S. Zhang, C. Liu, R. A. Gross, T. R. Kyriakides, W. M. Saltzman, *Biomaterials* **2011**, *32*, 6646.
[30] H. Bittiger, R. H. Marchessault, W. D. Niegisch, *Acta Crystallogr. Sect. B* **1970**, *26*, 1923.
[31] J. Cai, B. S. Hsiao, R. A. Gross, *Macromolecules* **2011**, *44*, 3874.
[32] G. Ceccorulli, M. Scandola, A. Kumar, B. Kalra, R. A. Gross, *Biomacromolecules* **2005**, *6*, 902.
[33] M. Gazzano, V. Malta, M. L. Focarete, M. Scandola, R. A. Gross, *J. Polym. Sci. Part B: Polym. Phys.* **2003**, *41*, 1009.
[34] P. Pan, Y. Inoue, *Progr. Polym. Sci.* **2009**, *34*, 605.
[35] W. Wagermaier, K. Kratz, M. Heuchel, A. Lendlein, *Adv. Polym. Sci.* **2010**, *226*, 97.
[36] J. D. Hoffman, R. L. Miller, *Polymer* **1997**, *38*, 3151.
[37] A. Kulkarni, J. Reiche, J. Hartmann, K. Kratz, A. Lendlein, *Eur. J. Pharm. Biopharm.* **2008**, *68*, 46.
[38] W. Small, T. S. Wilson, W. J. Benett, J. M. Loge, D. J. Maitland, *Opt. Express* **2005**, *13*, 8204.